J. Synchrotron Rad. (1999). **6**, 195–197

XAFS measurements on zinc chloride aqueous solutions from ambient to supercritical conditions using the diamond anvil cell

Robert A. Mayanovic[a], **Alan J. Anderson**[b], **William A. Bassett**[c], **and I-Ming Chou**[d].

[a] *Department of Physics and Astronomy, Southwest Missouri State University, Springfield, MO 65804, U.S.A.;* [b] *Department of Geology, St. Francis Xavier University, P.O. Box 5000, Antigonish, Nova Scotia B2G 2W5, Canada;* [c] *Department of Geological Sciences, Snee Hall, Cornell University, Ithaca, NY 14853, U.S.A.; and* [d] *MS 955 U. S. Geological Survey, Reston, VA 20192, U.S.A.*

The structure and bonding properties of metal complexes in subcritical and supercritical fluids are still largely unknown. Conventional high pressure and temperature cell designs impose considerable limitations on the pressure, temperature, and concentration of metal salts required for measurements on solutions under supercritical conditions. In this study, we demonstrate the first application of the diamond anvil cell, specially designed for x-ray absorption studies of first-row transition metal ions in supercritical fluids. Zn K-edge XAFS spectra were measured from aqueous solutions of 1-2*m* $ZnCl_2$ and up to 6*m* NaCl, at temperatures ranging from 25-660 °C and pressures up to 800 MPa. Our results indicate that the $ZnCl_4^{2-}$ complex is predominant in the 1*m* $ZnCl_2$/6*m* NaCl solution, while $ZnCl_2(H_2O)_2$ is similarly predominant in the 2*m* $ZnCl_2$ solution, at all temperatures and pressures. The Zn-Cl bond length of both types of chlorozinc(II) complexes was found to decrease at a rate of about 0.01 Å/100 °C.

Keywords: supercritical fluids, diamond anvil cell, chlorozinc complexes.

1. Introduction

The fluid structure of water changes significantly under sub- and supercritical conditions, due to progressive hydrogen bond breaking with increasing temperature. Consequently, the density, viscosity, and dielectric constant of water decrease with temperature. Hence, the solubility of many inorganic salts decreases, while for many organics it increases, in low-density supercritical water. The structure and bonding properties of inorganic complex species are directly dependent upon the solvation properties of water. However, exactly how these changes in the physical properties of water affect the nature of short-range interactions between ions at conditions from ambient to supercritical is still largely unknown. Determining the structure and speciation of complex ions is an essential step in developing a theoretical basis for solubility of ionic compounds and stability of ion complexes in sub- and supercritical water. The electronic structure theory of metal-ligand interactions is relatively well developed and least complicated for first-row transition metal ions, including zinc (Ballhausen, 1979). Hence, these metal ions when complexed with a ubiquitous ligand such as Cl^- can be used to study the effects of 3d electrons on their structure and stability in solutions. This has direct relevance to nuclear and chemical waste remediation using supercritical fluids (Shaw *et al.*, 1991), and hydrothermal geochemistry (Barnes, 1979; Crear *et al.*, 1985).

Conventional autoclaves have proven restrictive for studies on dissolved salts in supercritical water because of the severe corrosion problems caused by such fluids. The hydrothermal diamond anvil cell developed by Bassett *et al.* (1993) offers a much more suitable alternative because corrosion problems can be greatly minimized while control over pressure, temperature, and concentration can be substantially enhanced. However, x-ray absorption experiments have been limited to higher photon energies (> 15 keV) because of x-ray beam attenuation caused by the diamonds. By laser-drilling into the diamond anvils along the x-ray beam path, we have extended the workable photon energy range of the cell to less than 7 keV, using second-generation synchrotron sources. In this brief report, we describe our ongoing XAFS investigations on $ZnCl_2$/NaCl aqueous solutions from ambient to supercritical conditions using our modified diamond anvil cell.

2. Experimental

As part of a broader study on inorganic metal salts in aqueous solutions, our aim here was to investigate the effect of temperature (T), pressure (P), and Cl^- concentration on the structure and speciation of chlorozinc(II) complexes. Aqueous solutions of zinc chloride were prepared by pre-weighing reagent-grade powders of $ZnCl_2$ and NaCl, under dry atmosphere conditions. The powders were dissolved in deionized and distilled water. The Cl^- concentration in the solutions was controlled by adding specific amounts of NaCl. Three aqueous solutions were prepared, having the following (Cl:Zn) stoichiometric ratios: 2*m* $ZnCl_2$ (2:1) solution, 2*m* $ZnCl_2$ (3:1) solution, and 1*m* $ZnCl_2$ (8:1) solution. Each solution was placed in turn inside the sample chamber of the cell; the chamber was a 0.6 mm-diameter hole in either a 0.12 or 0.25 mm-thick Re gasket, sandwiched between two diamond anvil faces. The cell was heated by two separate resistance heaters, and the temperatures were measured using thermocouples placed on the anvils. The pressures of the solution inside the cell were accurately determined by P-T phase equilibria measurements, calibrated using the liquid-vapor homogenization temperature (Th_{L-V}) and the α-β quartz transition temperature (Bassett *et al.*, 1993).

Temperature- and pressure-dependent Zn K-edge x-ray absorption measurements were made on the zinc chloride solutions on beam line B2, at the Cornell High Energy Synchrotron Source (CHESS), in transmission mode. The storage ring at CHESS operated at 5.29 GeV, with a maximum stored current close to 220 mA. A double-crystal Si(111) monochromator detuned by 30-40 %, for rejection of higher harmonics, was used. The incident x-ray beam was collimated by fine slits to 250 x 250 μm. Four XAFS spectra were measured at each P-T point, for each solution. The diamond anvil cell was tilted by 0.1-0.2 degrees relative to the x-ray beam direction upon measurement of each of the first two of the set of four spectra, causing the diffraction peaks resulting from the diamonds to shift slightly in photon energy. This allowed for removal of the diffraction peaks from individual spectra using the "cut and paste" technique. The temperature was typically varied in roughly 100 °C increments from room temperature up to a maximum of 660 ± 4 °C, while the pressure varied according to the equilibrium vapor pressure for temperatures below Th_{L-V}. Above Th_{L-V}, pressures varied up to 800 MPa, depending upon the fluid density. The XAFS spectra were analyzed and fit using the combination of codes UWXAFS2.01 and FEFF6 (Mustre de Leon *et al.*, 1991). Fourier transforms of the $k^2\chi$ data were typically calculated in the k-range from 2.6 to 9.5-11 Å^{-1}, while r-space windows between 1.0-2.4 Å were used. It should be noted that the absorption edge energy value, determined by calculating the derivative in the edge region, was fixed during fitting.

3. Results

Representative $k^2\chi$ data, isolated from XAFS spectra measured under conditions ranging from ambient to 660 °C and 800 MPa, for the 2*m* $ZnCl_2$ (2:1) solution are shown in Figure 1: The corresponding Fourier transforms of the $k^2\chi$ data, along with transforms of the FEFF6 generated curves used in the fitting, are shown in Figure 2. The non-refined fitting results for these data shown in Table 1, indicate that the predominant chlorozinc(II) species in the solution is most likely $ZnCl_2(H_2O)_2$. We find that the number of Cl^- ligands (N_{Cl}) increases uniformly by 15-17% (just outside an error ± of 0.2.) with temperature. Conversely, the Zn-Cl bond length (R_{Zn-Cl}) exhibits a contraction of ~ 0.01 Å/100 °C, with an error of ± 0.007 Å, over the same P-T range. This is consistent with our results from previous studies of the structure of chlorozinc(II) complexes in saline fluid inclusions (Mayanovic *et al.*, 1997, Anderson *et al.*, 1998). Except for the Zn-O Debye-Waller factor (σ^2_{Zn-O}), the structure results for the water molecule ligands were less uniform over the same P-T range. This can in part be explained by the reduced backscattering amplitude of oxygen compared to the same for chlorine, for all values of wavevector k, thus making its signal more susceptible to distortion by noise. Common higher order cumulant expansion parameters (C_3 and C_4) were used in the fitting procedure to account for anharmonicity or non-Gaussian disorder of both the chlorine and oxygen radial distributions: The maximum values for these parameters are $C_3 = 1.6 \times 10^{-4}$ Å^3 and $C_4 = 4.4 \times 10^{-5}$ Å^4 from fitting of spectra measured at 660 °C and 800 MPa. Clearly, a more accurate accounting of such effects involves use of an individual set of cumulants C_3 and C_4 for the two types of ligands. Future work will involve such refinement in the fitting procedure. Comparison of structure results obtained from analysis of XAFS spectra measured at 440 °C and two different pressures, 30 and 200 MPa, showed that they are indistinguishable within the error bars. These results indicate that there is a dominant effect on speciation, trending towards a higher relative proportion of neutral $ZnCl_2(H_2O)_2$ complexes, in a manner consistent with previous solubility studies (Bourcier & Barnes, 1987; Cygan et al., 1994).

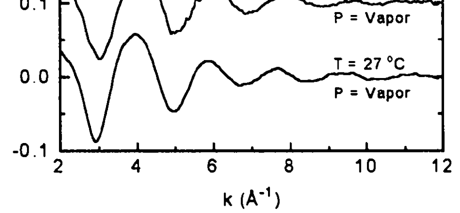

Figure 1

Representative isolated extended XAFS ($k^2\chi$) of the Zn K-edge spectra measured from a 2*m* $ZnCl_2$ (Cl:Zn = 2:1) aqueous solution, at P-T conditions ranging from ambient to 660 °C and 800 MPa.

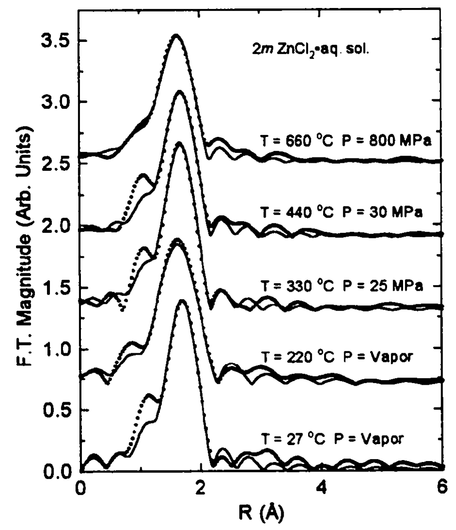

Figure 2

The magnitude of the Fourier transforms (FT) of the $k^2\chi$ data (points) shown in Figure 1, and of the fittings (solid lines) of these data, made using FEFF6 and a $ZnCl_2(H_2O)_2$ model.

Table 1

Fitting results for XAFS spectra measured from a 2*m* $ZnCl_2$ (Cl:Zn = 2:1) aqueous solution

T (°C)	P (MPa)	R_{Zn-Cl} (Å)	N_{Cl}	σ^2_{Zn-Cl} (Å^2)	R_{Zn-O} (Å)	N_O	σ^2_{Zn-O} (Å^2)
27	vapor	2.242	1.84	0.0039	2.053	1.5	0.004
110	vapor	2.230	1.93	0.0044	2.055	1.1	0.0039
220	vapor	2.214	1.95	0.0061	2.020	1.4	0.0056
330	25	2.202	2.01	0.0064	2.044	1.5	0.0064
440	200	2.196	2.18	0.0071	2.045	1.3	0.0068
550	175	2.186	2.14	0.0097	2.047	1.5	0.0094
660	800	2.178	2.09	0.0101	2.038	1.8	0.0106

Table 2
Fitting results for XAFS spectra measured from a 1*m* $ZnCl_2$ / 6 *m* NaCl (Cl:Zn = 8:1) aqueous solution

T (°C)	P (MPa)	$R_{Zn\text{-}Cl}$ (Å)	N_{Cl}	$\sigma^2_{Zn\text{-}Cl}$ ($Å^2$)	C_3 ($\times10^{-4}Å^3$)	C_4 ($\times10^{-5}Å^4$)	χ_r^2 †
27	vapor	2.295	3.81	0.0039	0.2	1.0	0.8
110	vapor	2.281	3.72	0.0052	4.4	5.0	0.82
220	vapor	2.269	3.86	0.0063	1.2	6.0	1.06
330	25	2.265	3.81	0.0072	1.9	9.0	0.99
385	200	2.260	3.63	0.0081	1.1	10.0	0.78
495	175	2.249	3.80	0.0097	3.5	9.0	1.15

† reduced chi-square or goodness of fit parameter

The structure results for the 1*m* $ZnCl_2$ (8:1) solution are shown in Table 2. It is evident from these results that the predominant zinc(II) complex in this P-T range is $ZnCl_4^{2-}$. As shown in Figure 3, the Zn-Cl bond length decreases uniformly with temperature, in a manner quite consistent with our previous results from studies on fluid inclusions (Mayanovic *et al.*, 1997, Anderson *et al.*, 1998) and results for the 2*m* $ZnCl_2$ (2:1) solution. Interestingly, the Zn-Cl bond length of the $ZnCl_4^{2-}$ complex appears to decrease in a non-linear fashion with increasing temperature. This result is consistent with how the physical properties of water, particularly the dielectric constant, vary with increasing temperature. Similar bond contraction results have been reported from XAFS studies on the first hydration shell of Rb^+ (Fulton *et al.*, 1996) and of Ag^+ (Seward *et al.*, 1996) in hydrothermal solutions.

Analysis of XAFS data measured from the 2*m* $ZnCl_2$ (3:1) solution, at temperatures ranging from 27 °C to 550 °C and pressures ranging from atmospheric to 360 MPa, is ongoing at the time of writing of this report. While it is presently clear that the Zn-Cl bond lengths decrease with increasing temperature in a manner consistent with results for the other two solutions, the nature of the chlorozinc(II) complexing is not entirely clear.

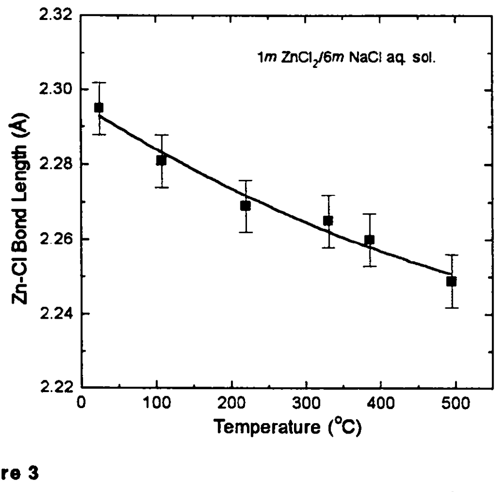

Figure 3
The dependence of the Zn-Cl bond length, of the $ZnCl_4^{2-}$ complex, in the 1*m* $ZnCl_2$ (Cl:Zn = 8:1) aqueous solution with temperature. The smooth curve, calculated by polynomial regression, is shown to aid the eye.

One possible mechanism responsible for bond contraction of the chlorozinc(II) complexes may be linked to water molecules, residing in the outer-hydration shell. Provided these waters interact with the Cl^- ligands through hydrogen bonding (Glendening & Feller, 1995), as the chlorozinc(II) complex becomes increasingly more dehydrated with temperature, breakage of water-ligand bonds occurs, resulting in stronger Zn-Cl bonding and thus a contraction of the same bond. If this is the actual mechanism responsible for the bond contraction, it may indicate that the strength of the complex-water molecule interaction, in the outer hydration shell, is stronger than what is presently deemed to be the case (Marcos *et al.*, 1991).

4. Conclusions

We have for the first time measured XAFS spectra from zinc chloride solutions using a diamond anvil cell specially designed for x-ray absorption studies of first-row transition metal ions in supercritical fluids. Our results indicate that the $ZnCl_4^{2-}$ complex is predominant in the 1*m* $ZnCl_2$/6*m* NaCl (8:1) solution up to 495 °C and pressures of 175 MPa. While $ZnCl_2(H_2O)_2$ is similarly dominant in the 2*m* $ZnCl_2$ (2:1) solution, a trend towards charge neutrality was noted over a similar P-T range, in a manner consistent with results from solubility studies (Bourcier & Barnes, 1987; Cygan *et al.*, 1994). The Zn-Cl bond length of both types of chlorozinc(II) complexes decreases at a rate of about 0.01 Å/100 °C. Similar future work involving metal bromide complexes, which have the advantage of being investigated at both the cation and ligand (Br) K edges, may shed further light on a mechanism responsible for the bond contraction of these and other inorganic complexes.

References

Anderson, A. J., Mayanovic, R. A. & Bajt, S. (1998). *Can. Mineral.* **36**, 511-524.

Ballhausen, C. J. (1979). *Molecular Electronic Structures of Transition Metal Complexes.* New York: McGraw-Hill.

Barnes, H. L. (1979). *Geochemistry of Hydrothermal Ore Deposits*, edited by H.L. Barnes, pp. 404-460. New York: J. Wiley & Sons.

Bassett, W. A., Shen, A. H., Bucknam, M., & Chou, I-M. (1993). *Rev. Sci. Instr.* **64**, 2340-2345.

Bourcier, W. L. & Barnes, H. L. (1987). *Econ. Geol.* **82**, 1839-1863.

Crerar, D., Wood, S., Brantley, S. & Bocarsly, A. (1985). *Can. Mineral.* **23**, 333-352.

Cygan, G. L., Hemley, J. J. & D'Angelo, W. M. (1994). *Geochim. Cosmochim. Acta.* **58**, 4841-4853.

Fulton, J. L., Pfund, D. M., Wallen, S. L., Newville, M., Stern, E. A., & Ma, Y. (1996). *J. Chem. Phys.* **105**, 2161-2166.

Glendening, E. D. & Feller, D. (1995). *J. Phys. Chem.* **99**, 3060-3067.

Mayanovic, R. A., Anderson, A. J. & Bajt, S. (1997). *Mater. Res. Soc. Proc.* **437**, 201-206; (1997). *J. Phys. IV France* 7, C2-1029-1030.

Marcos, E. S., Pappalardo, R. R. & Rinaldi, D. (1991). *J. Phys. Chem.* **95**, 8928-8932.

Mustre de Leon, J., Rehr, J. J., Zabinsky, S. I. & Albers, R. C. (1991). *Phys. Rev. B* **44**, 4146-4156.

Seward, T. M., Henderson, C. M. B., Charnock, J. M. & Dobson, B. R. (1996). *Geochim. Cosmochim. Acta.* **60**, 2273-2282.

Shaw, R. W., Brill, T. B., Clifford, A. A., Eckert, C. A. & Franck, E. U. (1991). *Chem. Engin. News*, **69**(51), 26-39.

(Received 10 August 1998; accepted 28 January 1999)